Journal of Applied Polymer Science

Conformational, Thermal, and Ionic Conductivity Behavior of PEO in PEO/PMMA Miscible Blend: Investigating the Effect of Lithium Salt

Mahdi Ghelichi,[1] Nader Taheri Qazvini,[2] Seyed Hassan Jafari,[1] Hossein Ali Khonakdar,[3] Yaser Farajollahi,[1] Christina Scheffler[4]

[1]School of Chemical Engineering, College of Engineering, University of Tehran, P.O. Box 11155-4563, Tehran, Iran
[2]Polymer Division, School of Chemistry, College of Science, University of Tehran, P.O. Box 14155-6455, Tehran, Iran
[3]Department of Polymer Processing, Iran Polymer and Petrochemical Institute, P.O. Box 14965-115, Tehran, Iran
[4]Department of Composite Materials, Leibniz Institute of Polymer Research Dresden, Hohe Str. 6, D-01069, Dresden, Germany
Mahdi Ghelichi and Yaser Farajollahi contributed equally to this work.
Correspondence to: N. T. Qazvini (E-mail: ntaheri@ut.ac.ir)

ABSTRACT: In this research, influence of incorporating $LiClO_4$ salt on the crystallization, conformation, and ionic conductivity of poly(ethylene oxide) (PEO) in its miscible blend with poly(methyl methacrylate) (PMMA) is studied. Differential scanning calorimetry showed that the incorporation of salt ions into the blend suppresses the crystallinity of PEO. The X-ray diffraction revealed that the unit-cell parameters of the crystals are independent of the $LiClO_4$ concentration despite of the existence of ionic interactions between PEO and Li cations. In addition, the complexation of the Li^+ ions by oxygen atoms of PEO is investigated via Fourier transform infrared spectroscopy. The conformational changes of PEO segments in the presence of salt ions are studied via Raman spectroscopy. It is found that PEO chains in the blend possess a crown-ether like conformation because of their particular complexation with the Li^+ ions. This coordination of PEO with lithium cations amorphize the PEO and is accounted for suppressed crystallinity of PEO in the presence of salt ions. Finally, electrochemical impedance spectroscopy is used to characterize the ionic conductivity of PEO in the PEO/PMMA/$LiClO_4$ ternary mixture at various temperatures. © 2012 Wiley Periodicals, Inc. J. Appl. Polym. Sci. 129: 1868–1874, 2013

KEYWORDS: blends; batteries and fuel cells; structure-property relations

Received 7 June 2012; accepted 30 November 2012; published online 24 December 2012
DOI: 10.1002/app.38897

INTRODUCTION

Polymer electrolytes have been the topic of great interest mostly because of their novel technological applications such as fuel cells and high energy batteries.[1,2] Among various homopolymers studied, poly(ethylene oxide) (PEO) exhibits excellent ion transport properties due to its high concentration of electron pairs and rapid segmental dynamics.[3,4] Meanwhile, PEO attains high degree of crystallinity, approximately 60%, at room temperature. The crystallites that can also cluster into spherulites are made up of PEO helices.[5] It had been primarily imagined that the crystalline domains are responsible for ion transport by means of ion motion up and down the helices. Nevertheless, it was recognized by NMR spectroscopy that diffusion occurs predominantly over the amorphous phase.[6] As the amorphous phase is the major contributor to the conductivity, then reducing the degree of crystallinity of PEO-salt systems becomes an unique design objective for which various fruitful efforts have been reported. These studies generally incorporate the development of PEO-based electrolyte nanocomposites, copolymers, and blends.[7–9]

Polymer blends offer a practical and efficient way to fulfill novel requirements for material properties and applications. Physical properties of polymer blends can be constantly varied among those of the pure components without synthesis of new materials. PEO-based miscible blends such as PEO/poly(methyl methacrylate) (PMMA) have attracted much attention in recent studies.[10–12] In miscible blends with a large dynamical asymmetry, that is large difference in glass transition temperature (T_g) of two polymers, the low T_g component represents an accelerated dynamics.[13] Accelerated segmental dynamics of confined PEO chains in rigid PMMA matrix, $\triangle T_g$ of components ~180°C, was investigated by different groups.[10,14] The accelerated segmental dynamics is essential for the ion-carrying component to reach high-conductivity values. Moreover, rigid PMMA chains provide sufficient mechanical stability for the soft PEO segments to achieve improved mechanical performance for

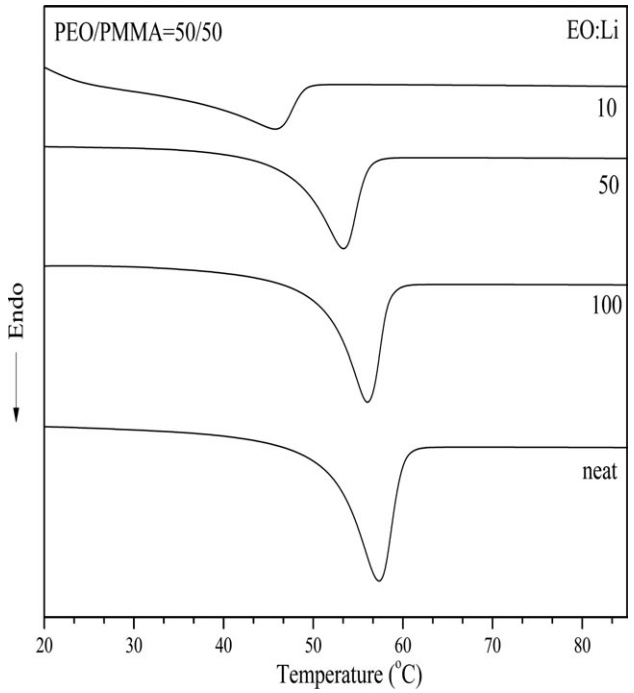

Figure 1. DSC thermograms for PEO/PMMA/$LiClO_4$ mixtures at various salt concentrations.

solid-state electrolyte applications. Therefore, PEO/PMMA miscible blend can be considered as an interesting candidate for use as electrolyte in solid-state lithium batteries. The miscibility of this blend is dependent on the tacticity of PMMA and the composition of the blends.[15,16] This system has been shown to be miscible up to a lower critical solution temperature of about 225°C.[17] It is reported that the conformation of PEO in PEO/PMMA blends is strongly perturbed by the presence of PMMA, which results in a conformational transformation from the gauche conformation (primarily a helical structure) to the trans conformation (leading to a planar zigzag structure) with the relative amount of trans sequences increasing with increasing PMMA content.[18–20]

Concerning the PEO electrolytes, vast amount of studies have been dedicated to investigating the thermal, conformational, and ionic properties of PEO-based nanocomposite and copolymer electrolytes, whereas there has been relatively very little research on PEO-based miscible polymer blend electrolytes. In this work, effect of adding salt ions of $LiClO_4$ on the thermal behavior, crystallinity, conformational change, and ion conductivity of PEO in the dynamically asymmetric miscible blend of PEO/PMMA is investigated through various methods.

EXPERIMENTAL

Materials and Sample Preparation

PEO ($M_w = 1 \times 10^5$ g mol^{-1} and $T_g = -67$°C) and PMMA ($M_w = 1.2 \times 10^5$ g mol^{-1} and $T_g = 114$°C) (catalog numbers: 181986, 182230, respectively, for PEO and PMMA) were purchased from Aldrich. The homopolymers were dried in complete vacuum for 24 h and stored in an argon-filled glovebox prior to blending. Lithium perchlorate ($LiClO_4$, battery grade) with a purity of 99.99% was supplied by Aldrich and was dried in a vacuum oven at 80°C for 24 h then put in a desiccator prior to use.

The composition of PEO/PMMA blend was 50/50 (wt./wt. %) and $LiClO_4$ was added to this blend according to the EO : Li values of 100, 50, and 10, resulting in one neat blend and three-doped blends with varying salt concentrations. Mixtures were prepared by dissolving three components in dichloromethane (DCM) and then stirring for 48 h. The solvent was then removed by casting and drying the solutions on Petri dish at room temperature for about 24 h. For complete removal of the solvent, the samples were vacuum dried at 77°C for another 24 h. Due to hygroscopic nature of PEO and $LiClO_4$, all the casting and drying processes were carried out in a glove box filled with argon gas.

Differential Scanning Calorimetry (DSC)

DSC measurements for investigation of nonisothermal crystallization behavior were performed on a Q2000 DSC (TA Instruments). The DSC thermographs were taken on the second heating (10°C min^{-1}) cycle after quenching from elevated temperature, ensuring that all the samples have the same thermal history. The samples were heated from −90 to 150°C under the atmosphere of dried N_2 and the sample weight was 5 mg in a sealed aluminum pan.

FTIR and Raman Measurements

Fourier transform infrared spectroscopy (FTIR) was performed using a Lincoln FTIR instrument at room temperature in the range of 400–4000 cm^{-1}.

X-ray Diffraction (XRD)

The XRD patterns for film samples were studied by using the X-ray diffractometer P4 with area detection system GADDS (Siemens AG Karlsruhe, now: BRUKER axs Karlsruhe) operating at 40 kV and 30 mA for Cu K_α radiation ($\lambda = 0.154$ nm). The scanning rate was 1° min^{-1} with a step size of 0.04° under the diffraction angle, 2θ, in the range of 1–40°.

Impedance Spectroscopy

Ionic conductivity measurements were performed for all samples using a custom made potentiostat. The ionic conductivity was determined by measuring the complex impedances of cells that are formed by sandwiching a given electrolyte sample with a thickness and diameter of 120 μm and 26 mm, respectively, between two blocking gold-coated copper electrodes. All measurements were carried out over the frequency range of 1 MHz to 0.1 Hz in a temperature-controlled chamber (±0.5°C). To allow for thermal equilibration, the samples were kept for 15 min at each temperature prior to the measurement.

RESULTS AND DISCUSSION

Figure 1 displays the DSC thermograms of PEO/PMMA/$LiClO_4$ mixture for different salt concentrations at the second heating scan. Heat capacity change (ΔC_p), $T_{m,PEO}$, $\Delta H_{m,\ PEO}$, $T_{g,PEO}$, and degree of crystallinity $X_{c,PEO}$, for all the samples are shown in Table I. The melting enthalpy, degree of crystallinity, and melting temperature of the blends all decrease with increasing the $LiClO_4$ content. In fact, addition of salt ions is found to

Table I. Thermal Properties of PEO in the Ternary Mixture of PEO/PMMA/$LiClO_4$

EO : Li ratio	ΔC_p (J g^{-1} K^{-1})	$\Delta H_{m,PEO}$ (J g^{-1})	$T_{m,PEO}$ (°C)	$T_{g,PEO}$ (°C)	$X_{c,PEO}$ (%)
0	0.53	35.2	57	−48	16.5
100	0.43	28.7	55	−46	13.4
50	0.42	25.3	53	−46	11.8
10	0.39	23.3	46	−41	10.9

reduce the crystallinity of PEO in the PEO/PMMA. As can be seen in Table I, the glass transition of PEO ($T_{g,PEO}$) gradually increases upon addition of salt ions. This T_g is probably due to the existence of a PEO-rich phase,[21] or because of the effective glass transition of low-T_g component in binary miscible blend.[22] Observed increase in $T_{g,PEO}$ reveals that the complexation of PEO with Li^+ ions has resulted in reduced chain mobility of PEO chains. This complexation is due to the formation of a coordinate bond between the ether–oxygen of the polymer and the cation of the salt. Wieczorek et al.[23] have previously observed this phenomenon and attributed retarded dynamics of PEO in the presence of salt ions to the temporary crosslinking provided by Li^+ ions. The degree of crystallinity (X_c (%)) of the polymer salt complexes can be calculated by considering the enthalpy of melting, that is, the area under the melting peak using the following equation:

$$X_c = \left(\frac{\Delta H}{\Delta H_0}\right) \times 100 \quad (1)$$

where ΔH is the enthalpy of melting of polymer metal salt complex and ΔH_0 (213.7 J g^{-1}) is the enthalpy of melting of 100% crystalline PEO.[24] According to the calculated X_c (%) values, incorporation of salt ions into the miscible crystalline blend of PEO/PMMA results in reduced degree of crystallinity of PEO. Diminishing the crystallinity of a crystalline polymer in the presence of salt ions was previously observed, however, establishing a relation between this phenomenon and the chain-level conformational changes was rarely attempted.

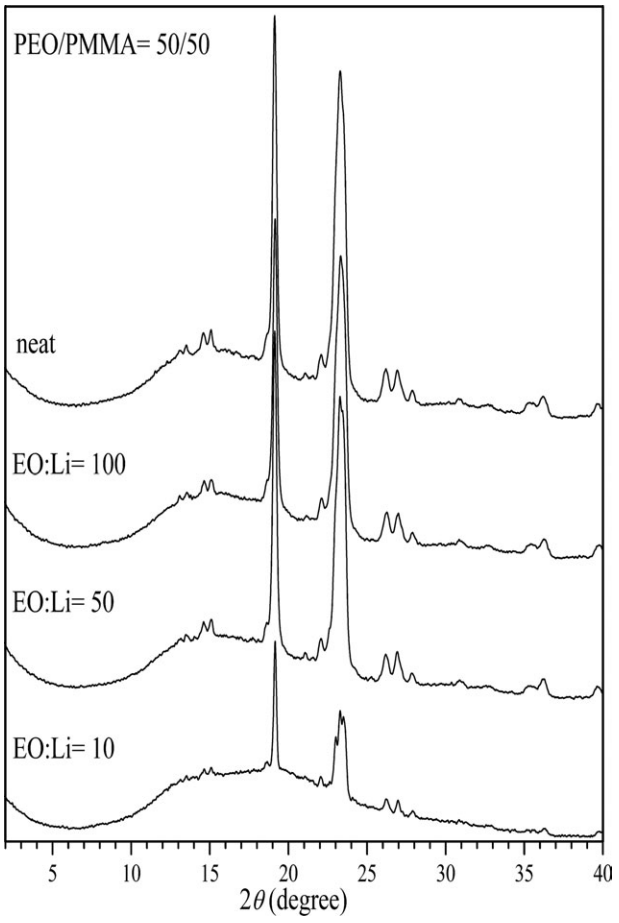

Figure 2. XRD patterns of PEO in PEO/PMMA and PEO/PMMA/$LiClO_4$ ternary mixtures at different EO : Li values.

Figure 2 represents the XRD patterns for PEO/PMMA blend and its blend/salt complexes. PEO/PMMA demonstrates two prominent diffraction peaks with diffraction angles 2θ close to 19 and 23.5° which are the characteristics of crystalline PEO.[19,25] The unit cell parameters can be resolved by combination of Bragg's equation and the equation for monoclinic crystal lattices.

$$n\lambda = 2d_{hkl}\sin\theta \quad (2)$$

$$\frac{1}{d_{hkl}^2} = \frac{h^2}{a^2\sin^2\beta} - \frac{2hl\cos\beta}{ac\sin^2\beta} + \frac{l^2}{c^2\sin^2\beta} + \frac{k^2}{b^2} \quad (3)$$

where λ is the X-ray wavelength (0.15418 nm), θ is the diffraction angle, d_{hkl} is the interplanar distance of two parallel (hkl) surfaces, a is 0.805 nm, b is 1.304 nm, c is 1.948 nm, and β is 125°. The characteristic peaks of PEO are preserved in the case of the blend/salt mixtures. However, the intensity of the diffraction peaks is reduced upon addition of $LiClO_4$, which means the crystallinity of PEO is suppressed in the presence of salt ions. Besides this, several diffraction peaks that were evident in the neat PEO/PMMA are disappeared in the high-diffraction-angle region that can support disturbed crystallinity of PEO in

Table II. Unit-Cell Structure Parameters of PEO Crystals as Determined from XRD Measurements

EO/Li	a (Å)	b (Å)	c (Å)
pure	8.11	13.05	19.64
100	8.10	13.00	19.56
50	8.07	13.04	19.49
10	8.04	13.03	19.45

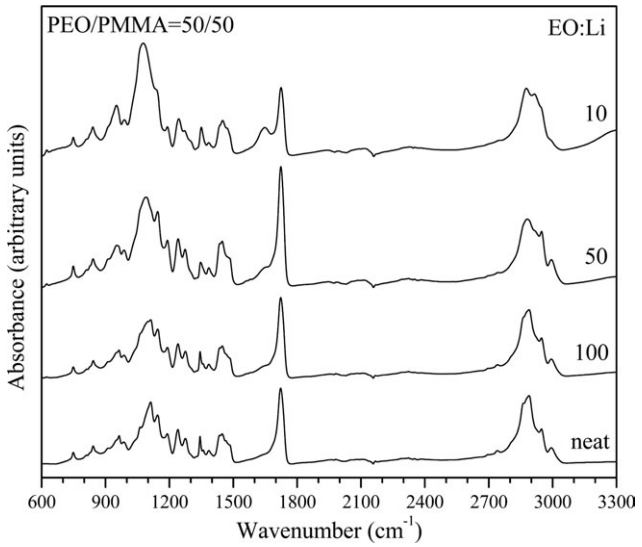

Figure 3. FTIR spectra from 600 to 3500 cm^{-1} for undoped and $LiClO_4$-doped specimens.

the miscible blend of PEO/PMMA/$LiCLO_4$.[26] Higher concentration of salt ions has also resulted in further repressed crystallinity of PEO chains. Suppressed crystallinity of PEO is in complete agreement with the DSC results. Observed decrease in the intensity of the peaks, as stated in Ref. 26, can be interpreted to confirm the formation of polymer-salt complex. It is clear that the peak positions from the XRD profiles are almost identical which indicates that the crystallizable PEO chains form a similar unit cell structure for the blends studied here. Based on the XRD data, the unit cell parameters of PEO crystals in its blend with PMMA and salt ions are calculated and presented in Table II. No variation is observed in the structure of crystals upon addition of $LiClO_4$ at different concentrations. Consequently, it can be understood that incorporation of salt ions

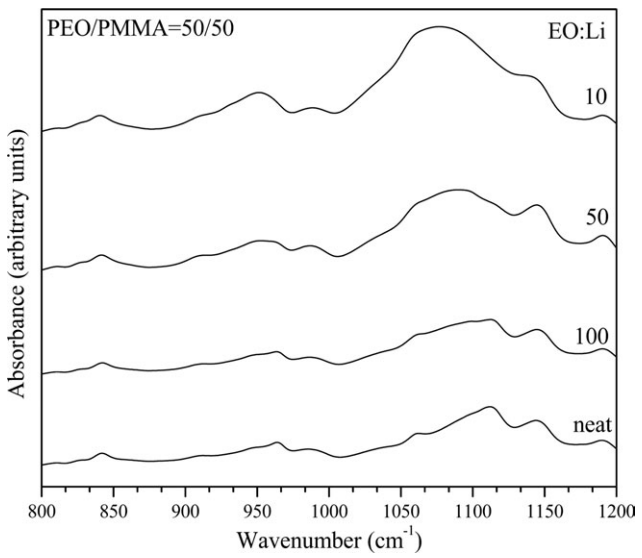

Figure 4. FTIR spectra of the samples in the spectral range of 800–1200 cm^{-1} (COC region).

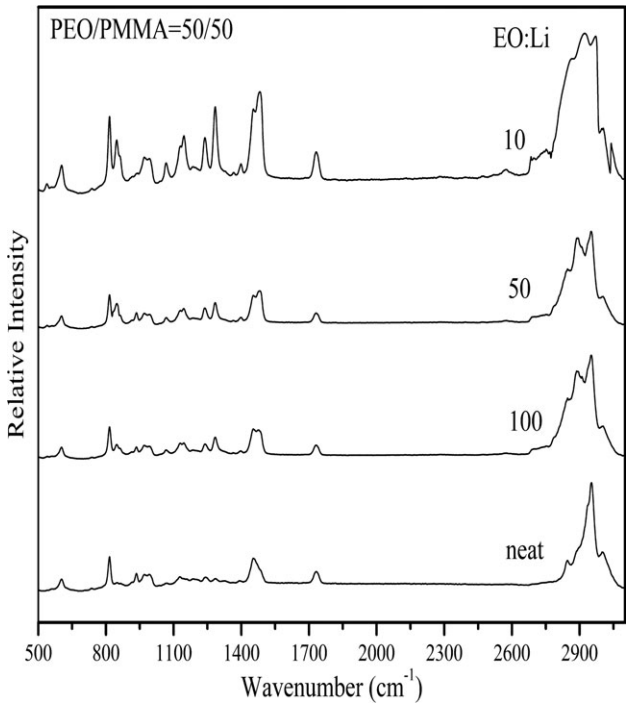

Figure 5. Raman spectra of the specimens in the range of 600–3000 cm^{-1} at different salt loadings.

partially amorphize the PEO chains and reduce the number of PEO chains taking part in the formation of crystalline domains while retain constant structure consistent with the pure PEO in the neat PEO/PMMA blend.

FTIR spectra of the neat PEO/PMMA and the $LiClO_4$-doped blends in the range of 600–3200 cm^{-1} are depicted in Figure 3. For better analysis, the FTIR spectrum of the samples in the 800–1200 cm^{-1} (COC region) is provided in Figure 4. The characteristic peaks of PEO at 1061, 1113, and 1145 cm^{-1} are clearly seen for the blend, but are barely eminent in the spectra of the $LiClO_4$-doped blends. The region from 1060 to 1150 cm^{-1} has been assigned to the contributions from CC stretching and COC stretching modes. In the case of coordination of alkali metal cation with the ether oxygens, large variations in this region can be expected.[27] Peak at 1113 cm^{-1} in the pure PEO/PMMA broadens and shifts toward lower wavenumbers in the case of polymer-salt complexes. The peak at 1145 cm^{-1} also follows the same trend. Changes in intensity, shape, and position of the COC stretching mode account for the complexation of Li^+ and PEO in the samples. Broad COC bands in the spectral region of COC indicate a low degree of crystallinity.[28] The restriction of crystallinity for high salt concentrations can also be shown by the flop in the duplet of the CH_2 wagging mode placed at 1340 and 1361 cm^{-1} in the blend, whereas it is a wide band located near 1350 cm^{-1} in the PEO/PMMA/$LiClO_4$ mixtures.[28] Peaks for pure $LiClO_4$ (1070 and 1610 cm^{-1}) vanish in the polymer complex which indicates that no additional salt exists in the complexes.[27]

Raman spectroscopy is carried out in an attempt to investigate the conformational changes of PEO by complexation with

Applied Polymer SCIENCE

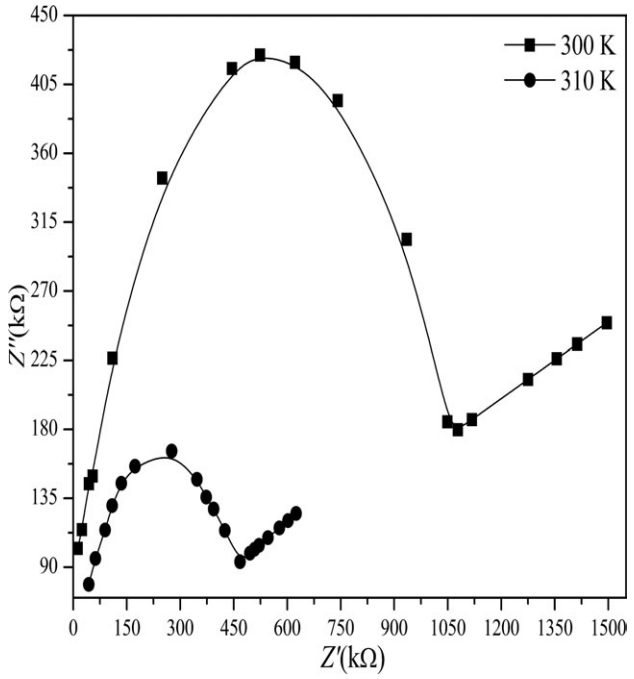

Figure 6. Variation of imaginary (Z'') with real (Z') part of impedance of PEO/PMMA/$LiClO_4$ with EO/Li = 50 at two different temperatures. Solid lines are a guide to the eye.

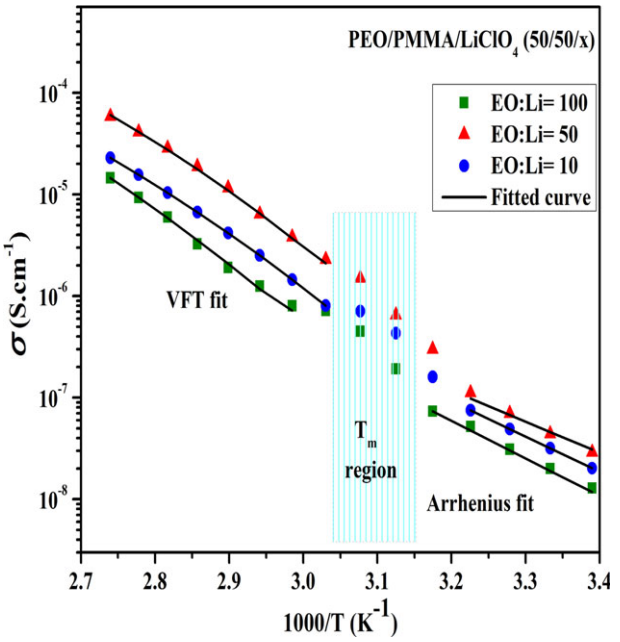

Figure 7. Temperature dependence plots of the ion conductivity of the doped blends at various EO/Li ratios. Solid lines below and above the T_m region are the Arrhenius and VFT fits to the date, respectively. [Color figure can be viewed in the online issue, which is available at wileyonlinelibrary.com].

$LiClO_4$ in the presence of PMMA. The Raman spectra of the neat PEO/PMMA blend and the salt-incorporated blends are shown in Figure 5. In 800–900 cm^{-1} range, ascribed to the rocking mode, the doped samples display discernible differences. In the system studied in this article, complexation prompts strong modifications of the broad νCH_2 shape of PEO on the way to give two relatively well-divided components. The latter can be associated with the ν_a and $\nu_s CH_2$ types of a crown ether-like local conformation around the cation. This is supported by the concurrent appearance of a Raman line at ~860 cm^{-1} which has been shown to be a characteristic of this kind of crown-ether conformation.[5,29,30] This Raman band has been assigned to the mode of PEO segment in which segments are able to solvate the lithium ion and adopt a kind of crown-ether conformation. As a result, complexation of PEO with Li^+ ions is estimated to favor the crown-ether like conformation of PEO chains in the miscible blend of PEO/PMMA. In the case of PEO/PMMA/$LiClO_4$ with various salt concentrations wider peaks indicate lower degrees of crystallinity, which are in agreement with the former measurements.

The complex impedance spectrum plots ($-Z''$ vs. Z') are used to determine the ionic conductivity of the polymer blend electrolytes. The impedance plot for a sample with EO/Li = 50 is shown at two different temperatures in Figure 6. All sample spectra are comprised of a semicircle in the high-frequency region followed by an inclined line in the region of lower frequency. The higher frequency semicircle describes the bulk properties of samples, but inclined line can be attributed to electrode polarization where the ions buildup near the electrodes at low frequencies. The bulk resistance (R_b) of the materials is determined from the intercept of the semicircle with the real axis (Z') at low frequency. Then, ionic conductivities were calculated using the equation:

$$\sigma = L/R_b A \tag{4}$$

where L is the thickness, R_b is the bulk resistance, and A is the known area of the electrolyte film. In Figure 7, the ionic conductivity of blends has been plotted as a function of temperature in the range of 295–363 K. As can be seen in all the blends, the conductivity σ increases by increasing the temperature, however, an intense variation is observed in the T_m region of the studied blends. It is currently accepted that the ionic conductivity in polymer electrolytes occurs in the amorphous phase where the ion conduction is mediated by local motion of the polymer chain segments above T_g.[31] The intensive increase of conductivity close to T_m can be attributed to the increment of amorphous phase and consequent enhancement in segmental mobility. To have better insight into the temperature dependence of σ, the fitting of the experimental data are attempted.

Table III. Arrhenius Fitted Parameters from the Temperature Dependence of the Conductivity Below the T_m

EO/Li	log A	E_a (eV)
100	4.618	0.733
50	2.825	0.604
10	4.1	0.69

Table IV. VFT Fitted Parameters from the Temperature Dependence of the Conductivity Above the T_m

EO/Li	σ_0	E_v (eV)	T_0 (K)
100	0.6	0.189	203
50	0.048	0.111	230
10	0.091	0.149	211

In all the blends below the T_m, the data are fitted with Arrhenius equation:

$$\sigma = A \ \exp(-E_a/\mathrm{RT}) \tag{5}$$

where A is a preexponential factor and E_a is the activation energy. These fitting values, log A and E_a, are listed in Table III for different samples. For upper T_m region, the behavior is comparatively different. In all samples, the conductivity data in upper T_m are fitted to the Vogel–Fulcher–Tamman (VFT) equation of the form:[31]

$$\sigma = \sigma_0 T^{1/2} \ \exp(-E_v/K(T - T_0)) \tag{6}$$

where σ_0 is the prefactor, T is the absolute temperature, K is the Boltzmann constant, E_v is the pseudo-activation energy, and T_0 is the equilibrium glass transition temperature at which the free volume disappears. The finest fitted parameters, σ_0, E_v, and T_0 are shown in Table IV. VFT behavior has been explained invoking the concept of free volume.[32,33] This behavior demonstrates that PEO chains that are responsible for conduction of ions have liquid-like behavior. Also, the reasonably good fit of σ to VFT equation indicates that there is a close coupling between the ion conductivity and PEO segmental mobility, in the neighboring frozen PMMA chains. Our theoretical prediction was that conductivity increases with increasing salt concentration because of the increment of amorphous phase which is also seen in DSC and XRD results. However, as can be seen from Figure 6, blend with EO/Li = 10 shows conductivity lower than that of EO/Li = 50. This has been attributed to the ion-pairing at higher salt concentrations. Such behavior has also been reported for PEO-$LiCF_3SO_3$ solid electrolytes by Katiyar et al.[31] They reported that the conductivity increases with increasing salt concentration and reaches a maximum for EO/Li = 24 and after that the conductivity declines with further addition of salt. It seems that in our blends ion-pairing takes place for salt values lower than EO/Li = 50. The Arrhenius behavior observed below T_m may be attributed to the lower mobility of PEO segments in the amorphous phase confined between crystalline regions. However, supper-Arrhenius (VFT) behaviors were detected for temperatures higher than T_m due to the melting of crystals and consequently, speed up of segmental mobility.

Addition of small cations in the form of salt ions has been shown to reduce or completely destroy the crystallinity of PEO. In this work, this behavior is attributed to the strong coordination of PEO to small cations of Li^+, which promotes crown-ether type of backbone conformations. Strawhecker et al.[34] proposed that strong coordination of PEO to the surface of Na^+ cations supports noncrystalline (crown-ether) conformations of PEO which are highly amorphous. Papke et al.[5] studied the complexes of PEO with various alkali metal salts. It was proposed that cation-dependent vibrational bands observed in the far-IR and metal–oxygen (M[sbond]O_n) symmetric stretching bands support a cation-oxygen atom interaction and indicate that the polyether chain may possibly wrap around the cations. Indeed, complexes of PEO are believed to have a helical configuration which differs from the configuration of pure PEO. Such crown-ether conformations deviate from the helical PEO conformations typically found in bulk PEO crystals and therefore amorphize the PEO. In a computer simulation performed by Müller-Plathea et al.,[35] it was found that PEO prefers to act like a polydentate ligand when binding to Li^+ ions. Oxygens belonging to consecutive monomers coordinate to the same ion and the polymer chain is forced into loops which very much resemble crown ethers. In this work, incorporating salt ions is found not to affect the crystal structure of PEO while have reduced the degree of crystallinity of PEO in PEO/PMMA/ $LiClO_4$ mixture. The diminished crystallinity is attributed to the specific complexation of PEO segments with the Li^+ ions which favors the amorphous state of the PEO chains. Furthermore, the importance of the ion pair formations at high salt concentrations is discussed in the context of impedance spectroscopy.

CONCLUSIONS

From the DSC results, it was found that the crystallinity of the PEO component in PEO/PMMA blends decreases with the increase of the $LiCiO_4$ salt concentration. Reduced chain mobility of PEO chains because of the complexation with Li^+ ions has resulted in an increase in the glass transition of PEO. The overall crystallinity of PEO is reduced in the presence of salt ions, whereas the crystal structure of PEO is not disturbed at different salt concentrations. A crown-ether conformation, which favors the amorphous state of PEO is considered to be the primary reason of suppressed crystallinity of PEO. Through electrochemical analysis, it is found that ion-pairing effect which usually appears at high salt concentrations is observed in the case of doped blend with EO : Li of 10. The close coupling between the ionic conductivity and the segmental flexibility of PEO is achieved according to a reasonable fit of conductivity data to VFT equation. The observed Arrhenius behavior below T_m of the PEO in the blend is attributed to the lower mobility of PEO segments in amorphous phase, which are restrained between crystalline regions. For the temperatures higher than T_m a supper-Arrhenius (VFT) behavior is perceived and is considered as a result of melting crystals and accelerated segmental dynamics.

REFERENCES

1. Zhang, H.; Shen, P. K. *Chem. Rev.* **2012**, *112*, 2780.
2. Agrawal, R. C.; Pandey, G. P. *J. Phys. D: Appl. Phys.* **2008**, *41*, 223001.
3. Chandrasekaran, R.; Selladurai, S. *J. Solid State Electrochem.* **2001**, *5*, 355.

4. Acosta, J. L.; Morales, E. *J. Appl. Polym. Sci.* **1996**, *60*, 1185.
5. Papke, B. L.; Ratner, M. A.; Shriver, D. F. *J. Phys. Chem. Solids* **1981**, *42*, 493.
6. Berthier, C.; Gorecki, W.; Minier, M.; Armand M. B.; Chabagno, J. M.; Rigaud, P. *J. Solid State Ionics* **1983**, *11*, 91.
7. Manoratne, C. H.; Rajapakse, R. M. G.; Dissanayake, M. *Int. J. Electrochem. Sci.* **2006**, *1*, 32.
8. Young, W. -S.; Epps, T. H. *Macromolecules* **2009**, *42*, 2672.
9. Chiu, C. -Y.; Chen, H. -W.; Kuo, S. -W.; Huang, C. -F.; Chang, F. -C. *Macromolecules* **2004**, *37*, 8424.
10. Brodeck, M.; Alvarez, A.; Moreno, A. J.; Colmenero, J.; Richter, D. *Macromolecules* **2012**, *45*, 536.
11. Jeddi, K.; Taheri Qazvini, N.; Jafari, S. H.; Khonakdar, H. A.; Seyfi, J.; Reuter, U. *J. Polym. Sci. Part B: Polym. Phys.* **2011**, *49*, 318.
12. Osman, Z.; Ansor, N. M.; Chew, K. W.; Kamarulzaman, N. *Ionics* **2005**, *11*, 431.
13. Lutz, T. R.; He, Y.; Ediger, M. D.; Cao, H.; Lin, G.; Jones, A. A. *Macromolecules* **2003**, *36*, 1724.
14. Tyagi, M.; Arbe, A.; Colmenero, J.; Frick, B.; Stewart, J. R. *Macromolecules* **2006**, *39*, 3007.
15. Dionisio, M.; Fernandes, A. C.; Mano, J. F.; Correia, N. T.; Sousa, R. C. *Macromolecules* **2000**, *33*, 1002.
16. Hamon, L.; Grohens, Y.; Soldera, A.; Holl, Y. *Polymer* **2001**, *42*, 9697.
17. Fernandes, A. C.; Barlow, J. W.; Paul, D. R. *J. Appl. Polym. Sci.* **1986**, *32*, 5481.
18. Li, X.; Hsu, S. L. *J. Polym. Sci. Part B: Polym. Phys.* **1984**, *22*, 1331.
19. Shieh, Y. -T.; Liu, K. -H. *J. Polym. Sci. Part B: Polym. Phys.* **2004**, *42*, 2479.
20. Ramana Rao, G.; Castiglioni, C.; Gussoni, M.; Zerbi, G.; Martuscelli, E. *Polymer* **1985**, *26*, 811.
21. Lin, J. -H.; Woo, E. M.; Huang, Y. -P. *J. Polym. Sci. Part B: Polym. Phys.* **2006**, *44*, 3357.
22. Wieczorek, W.; Raducha, D.; Zalewska, A.; Stevens, J. R. *J. Phys. Chem. B* **1998**, *102*, 8409.
23. Jingyo, X.; Tang, X. *J. Electrochim. Acta* **2006**, *51*, 4765.
24. Marcos, J. I.; Orlandi, E.; Zerbi, G. *Polymer* **1990**, *31*, 1899.
25. Money, B. K.; Hariharan, K. *Appl. Phys. A* **2007**, *88*, 647.
26. Lodge, T. P.; McLeish, T. C. B. *Macromolecules* **2000**, *33*, 5278.
27. Rajendran, S.; Mahendran, O.; Kannan, R. *J. Solid State Electrochem.* **2002**, *6*, 560.
28. Roccoa, A. M.; Fonsecab C. P.; Loureiroa F. A. M.; Pereira, R. P. *Solid State Ionics* **2004**, *166*, 115.
29. Fouassier, M.; Lassegues, J. C. *J. Chem. Phys.* **1978**, *75*, 865.
30. Rey, I.; Lasseagues J. C.; Grondin, J.; Servant, L. *J. Electrochim. Acta* **1998**, *43*, 150.
31. Karan, N. K.; Pradhan, D. K.; Thomas, R.; Natesan, B.; Katiyar, R. S. *J. Solid State Ionics* **2008**, *179*, 689.
32. Cohen, M. H.; Turnball, D. *J. Chem. Phys.* **1959**, *31*, 1164.
33. Grest, G. S.; Cohen, M. H. *Phys. Rev. B* **1980**, *21*, 4113.
34. Strawhecker, K. E.; Manias, E. *Chem. Mater.* **2003**, *15*, 844.
35. Müller-Plathea, F.; van Gunsteren, W. F. *J. Chem. Phys.* **1995**, *103*, 4745.